

Practical applications of seismic anisotropy

Philip Wild, Ikon Science Inc., Teddington, United Kingdom
pwild@ikonscience.com

Summary

Although generalizations can be unfair and controversial, it is helpful to divide interest in seismic anisotropy into one of two broad categories: situations where anisotropy is an inconvenience and must be removed or corrected for in an analysis, and applications where anisotropy can be exploited to improve an interpretation. For those requiring a sub-surface image, especially using wide-azimuth and far-offset seismic data, anisotropic effects must be considered in the processing flow to remove anomalies caused by directional variations in the seismic velocity. For a quantitative interpretation, there is significant potential information that the anisotropy can reveal what is well worth exploiting, especially about fracturing.

Introduction

The review has not set out to give a summary of anisotropic theory; several publications already cover this from mathematical and explorational viewpoints, for example Thomsen (1986 and 2002), Winterstein (1990), and Tsvankin (2005). The following two definitions are sufficient here: anisotropy can be defined as 'a variation of a physical property depending on the direction in which it is measured' (Sheriff, 2002) and more specifically, seismic anisotropy is defined as 'the dependence of seismic velocity upon angle' (Thomsen, 2002). Additionally, only a small number of seismic anisotropy types are needed to make reasonable headway in understanding and gaining use from the phenomenon (Figure 1). The simplest two of these anisotropies, vertical transverse isotropy (VTI) for characterizing horizontal layering, such as in shale sequences, and horizontal transverse isotropy (HTI) for characterizing vertical fracturing, will be considered in the examples below.

Well ties

Within the modern exploration and production environment, tying wells to seismic is the crucial step to interpretation, inversion, and subsurface analysis. There is a growing need to tie wells to seismic with greater accuracy and more frequently than ever before, which has been driven by the increasing use of quantitative interpretation and rock property extraction from seismic data. Standard structural interpretation can proceed with well ties using wavelets of up to 30° of phase error. Seismic inversion, however, must have wavelets with phase errors of less than 10°, in order to reproduce impedance steps correctly and of high enough consistency that they can be averaged to create a single wavelet for a 3D survey.

In Wild, et al. (2008), a procedure is described to improve the tie between synthetics derived from borehole recorded velocities and the surface seismic data. Anisotropy is included in the synthetic model in two ways, firstly by verticalizing the borehole derived velocities to match their deviated propagation direction to the vertical velocity direction which is used in the processing of the surface seismic data. Secondly, anisotropic formulations for reflectivity coefficient calculations using theory

from Vavryčuk and Pšenčík (1998) and Jilek (2000), amongst others, are used in place of isotropic formulations.

The verticalization issue is emphasised by comparing track (g) of Figure 2, which shows the poor match of the synthetic (computed from deviated bore-hole velocities) to the surface seismic (tracks f and i), with the much improved synthetic in track (k), which gives a good correlation with the near and far recorded traces because this synthetic has been computed using the derived vertical velocities. Here the reservoir contains near-vertical fractures which we modelled as HTI anisotropy using theory from Hudson (1981) and Schoenberg and Sayers (1995); the different velocities are attributed to the anisotropy, which gives faster P-waves for vertical propagation (stiffer rock in-line with the fracture strike) compared to deviated directions which contain an element of the fracture's normal compliance.

The methodology of verticalizing well velocities has been applied in a number of fields and for different anisotropies, and is an example where the seismic anisotropy should be corrected to ensure synthetics and seismic have been computed and processed using the same velocities.

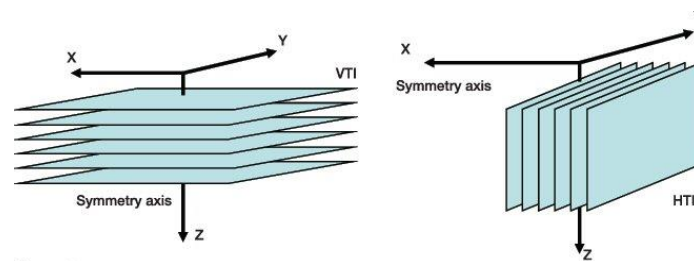


Figure 1: VTI anisotropy (left) characterizes horizontal layering, as evidenced in shale overburdens. The stiffening of the rock in the horizontal direction increases the P-wave velocity in this direction compared to vertical propagation. HTI anisotropy (right) characterizes vertical fracturing, such as seen in a fractured reservoir. Here the rock is stiffer along the strike of the fractures giving the fastest P-wave velocity in this direction.

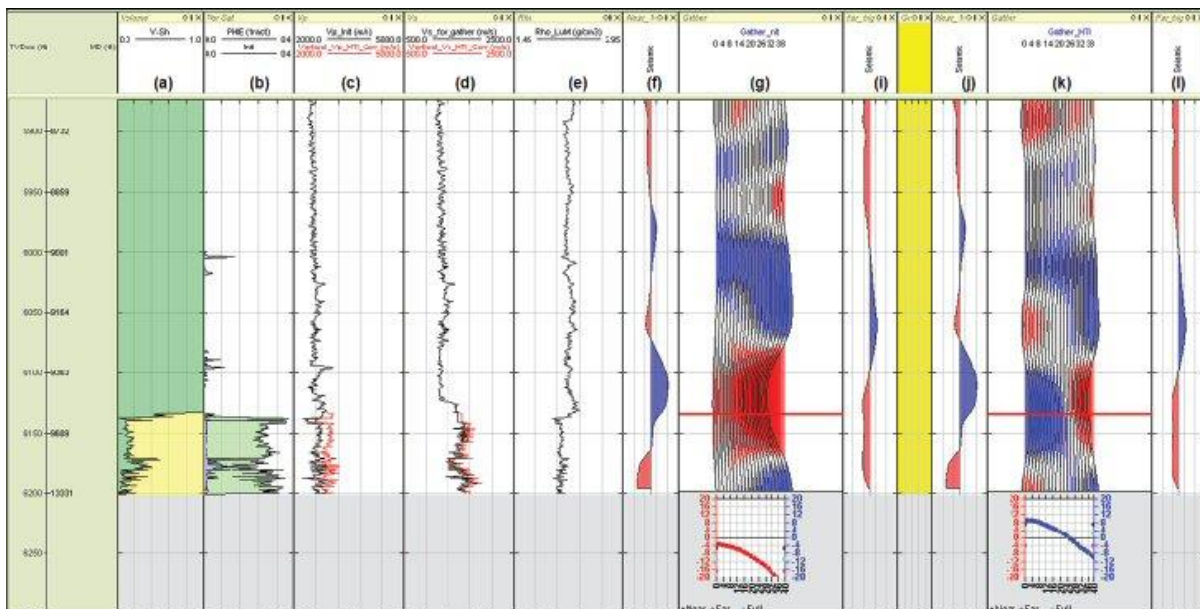


Figure 2: Two synthetic traces are displayed alongside corresponding composite traces extracted along the deviated well-bore path from a seismic data volume. The synthetic gather in track (g) has been computed using raw log velocities and is poorly correlated with the near stack trace (track f); whereas the synthetic in track (k) has been computed using verticalized velocities and an anisotropic model and correlates well with the near (j) and far stack traces (l). The red curves in (c) and (d) show the verticalized V_p and V_s , which for vertical fractured

media will tend to have higher values than their deviated counterparts shown in black; other tracks show shale volume (a), porosity (b) and density (e).

Overburden

Knowledge of the anisotropy in the overburden, which as a first approximation is assumed to be made up of horizontal layering (characterized by VTI anisotropy) is of particular importance when building velocity models. The rock matrix is stiffer along bounds of the layering and it is not unusual for the horizontal velocity to be some 10% faster than in the vertical direction. Where the layering is flat, the anisotropy is constant with azimuth (hence the term polar anisotropy may be used for VTI), but when the layering dips, or is also fractured, the situation becomes more complicated.

Several methods are employed to compute the overburden anisotropy, including sonic logging (on a local scale), ray trace modelling, and walk-away VSPs. A field example of the use of a walk-away VSP is shown in Figure 3. Here a number of shots have been fired along a horizontal line into receivers located at regular intervals down a borehole. The acquired data are then sorted and processed into shot and receiver gathers, from where vertical slowness (inverse velocity) and horizontal slowness values are computed for each shot/receiver pair. Finally these slowness values are inverted by solving the P-wave anisotropy velocity equation (Thomsen 1986) to yield terms for the anisotropy (Figure 4).

Other inversion schemes exist for walk-away data, such as inverting with the P-wave polarization angle variation with offset in place of horizontal slowness (Grechka, et al., 2007) and using 3D VSP data to invert for both layering and fracture induced anisotropy (Owusu, et al., 2011). In theory, the walk-away VSP can be used to invert shear-waves to yield an estimate of the shear-wave anisotropy; in practice, this is much more difficult due to the noisy nature of the shear-wave arrival.

The output from these inversion schemes is generally in terms of Thomsen's (1986) ϵ , γ , and δ parameters, which account for the P and shear anisotropy in the model. These values, which are sufficient for describing the simplest cases of VTI (and HTI) anisotropy, can be passed into velocity models used in move out and migration steps for processing associated surface seismic data (for example, Close, et al., 2010).

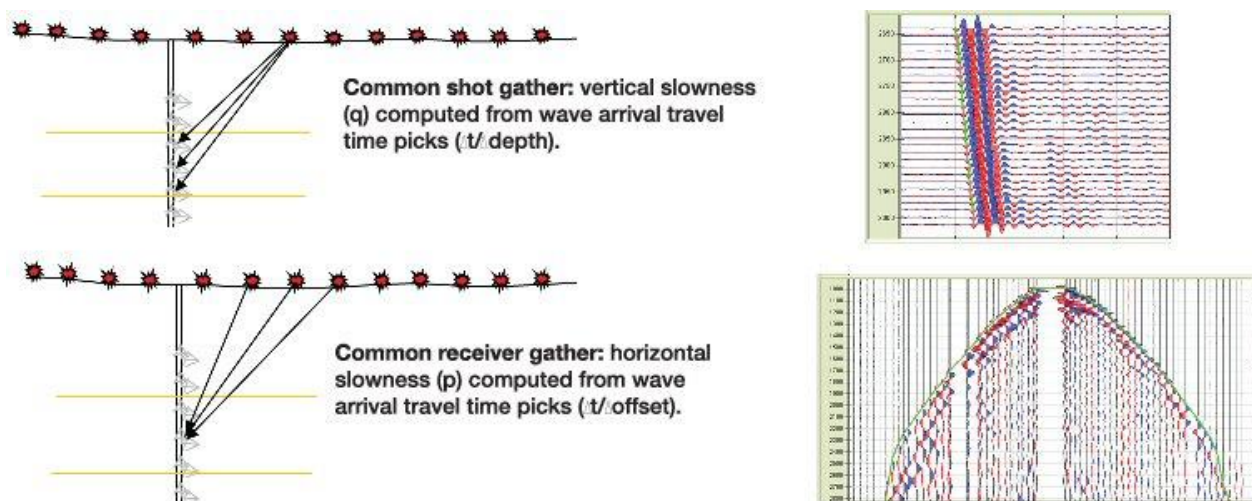


Figure 3: The geometry of a walk-away VSP showing the how data from receivers and shot points are arranged to yield vertical and horizontal slowness values. Example shot and receiver gathers are shown on the right.

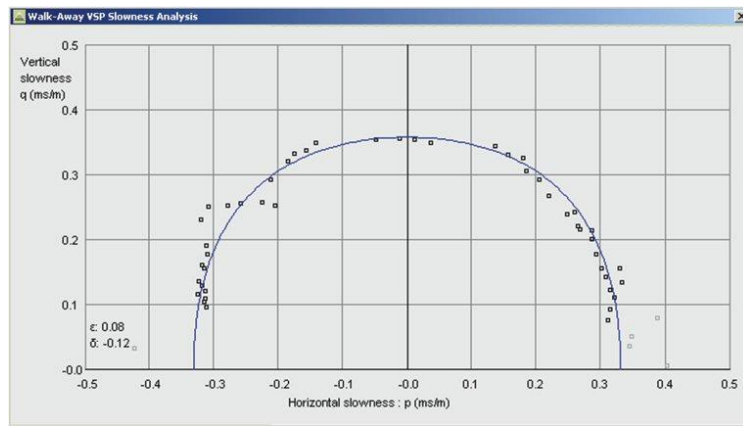


Figure 4: The Thomsen (1986) parameters describing the P-wave anisotropy, ϵ and δ , are inverted by fitting a curve to the walk-away VSP derived horizontal and vertical slowness values using an anisotropic velocity equation (Thomsen 1986).

Fractures -azimuthal variations

Having considered two applications of anisotropy that enable improved imaging, approaches for exploiting anisotropy for the analysis of fractured formations are worthy of discussion. One uses azimuthal variations in the amplitude versus offset (AVO) signature when the wave is reflected from the top or base of an anisotropic material, and a second exploits the polarizing effect that the fractures have on a transmitted shear-wave. In both cases, the individual fractures are below the resolving power of the seismic signal and it is the cumulative effect of the fracturing that is recorded.

Plots in Figure 5 show how the amplitude of a reflected signal varies with both offset and azimuth, with the signal measured at the interface between an upper isotropic shale layer and a lower sandstone layer. The sandstone layer may either be set to isotropic, or else vertically fractured, in which case it is represented by 10% HTI anisotropy (that is the velocity normal to the fracture strike is 90% of the velocity parallel to the strike). At an incidence angle of 25° the P-wave reflectivity response at the top of the fractured sandstone (Figure 5 upper plot, right hand black curve) shows an elliptical shape as the observation azimuth is varied, with an increase in the reflectivity values at an azimuth normal to the fracture strike compared to the equivalent isotropic response (grey line). Even so, the comparative AVO response between the two models is very similar for a fixed observation angle.

The P to shear (PS) reflected signal is more complicated: for the anisotropic model there are two reflected shear components, one polarized parallel to the vertical (PSv), shown in cyan (Figure 5, lower) and the other polarized parallel to the horizontal direction (PSh), shown in magenta. Both these signals show a more pronounced variation compared to the isotropic model (grey). A key conclusion to take away from this modelling is that the PS signal is more sensitive to the fracturing than the corresponding PP signal, and that it is worth exploring the possibility of acquiring shear data in the field. This observation is evident when looking at a series of synthetic gathers computed from PP and PSv reflectivity values at the top of the fractured sandstone layer (Figure 6). There is a similar slight dimming of the PP signal for both isotropic and anisotropic gathers (left pair of tracks), but a more pronounced brightening of the signal for the PS anisotropic gather compared to the PS isotropic gather (right pair of tracks).

Several methods are available to invert these azimuthal AVO responses, with the general requirement being that the AVO response has to be measured along more than one azimuthal direction. VSPs provide one way of achieving a good range in offset, with several walk-away lines at different angles. For surface seismic data it is questionable whether sufficient azimuthal coverage

can be achieved, especially in a marine environment (see section on acquisition design below) where long-offset reflections are required. OBC has had better success (Vetri, et al., 2003) where both P and shear waves have been inverted to yield fracture strike and fracture density.

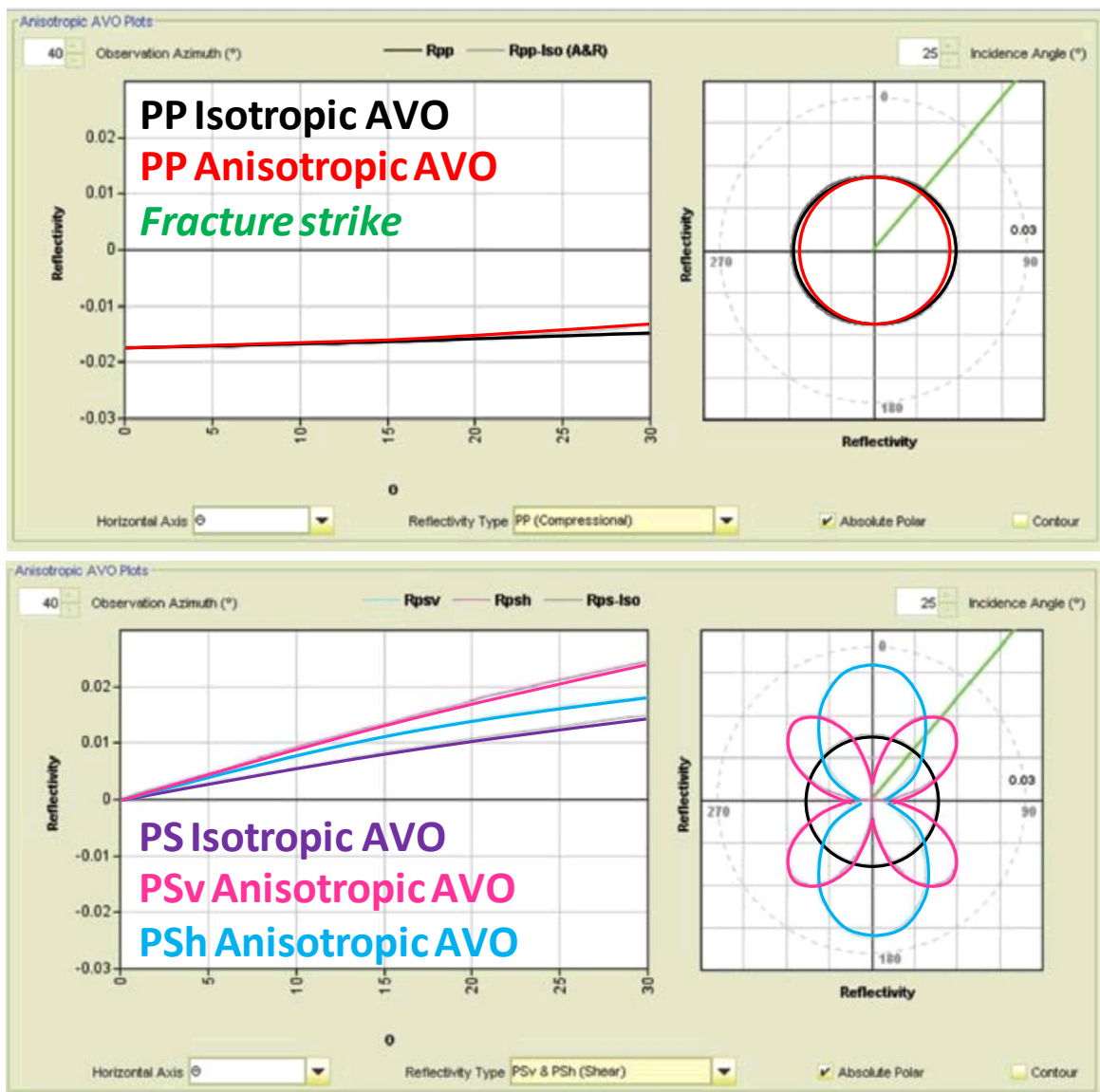
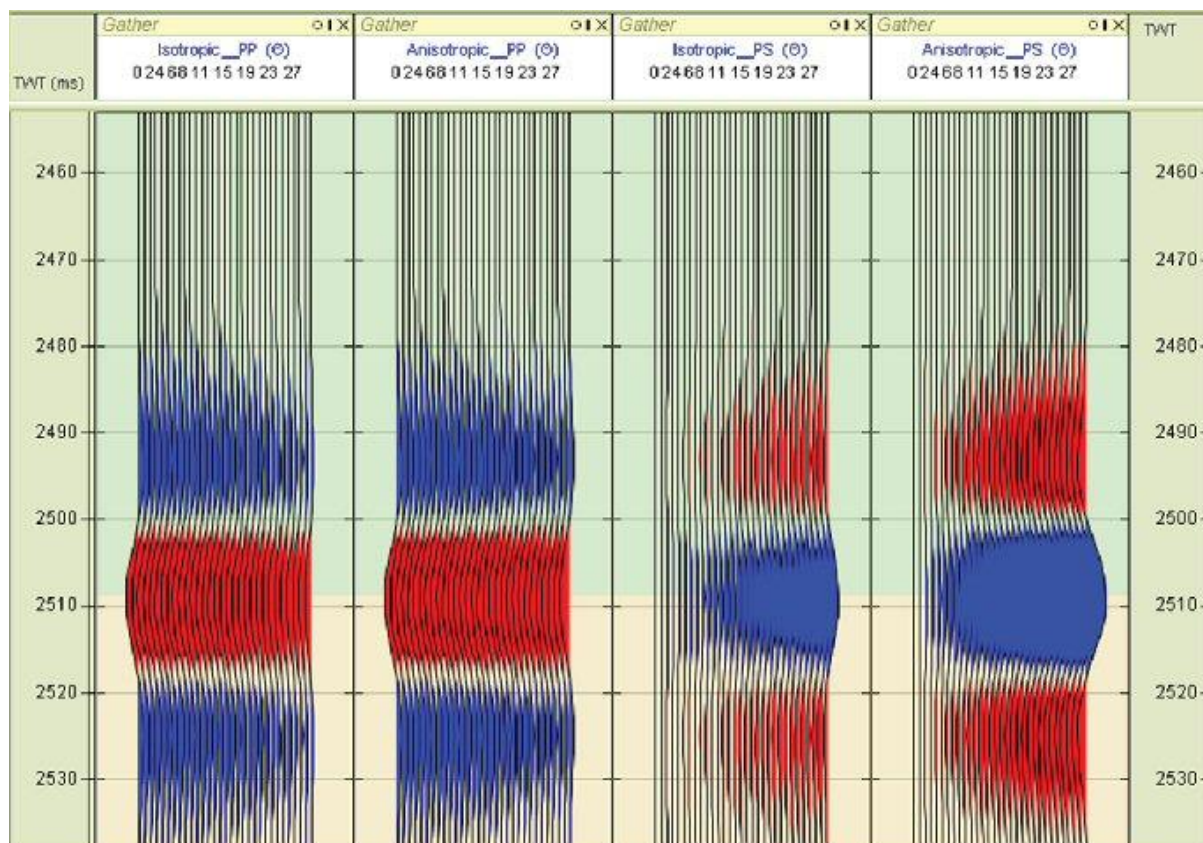


Figure 5: A blocky model is constructed using a shale layer (assumed isotropic) over a lower vertically fractured sand layer (HTI, approximately 6% anisotropy). Upper plot is the PP AVO response (black anisotropic and grey for a purely isotropic response), with the left graph showing amplitude against offset at an observation azimuth of 40° to the fracture strike (assumed North/South). The azimuthal trend in the reflectivity values at a constant offset of 25° is shown on the right, highlighting the small difference between the anisotropic (black) and isotropic (grey) values. Lower plot is the equivalent PS AVO response, with PSv (cyan) and PSh (magenta) reflectivities. Note the anisotropy PS reflectivity values show a much greater difference from their equivalent isotropic values compared to the PP.

Another solution is to use a walk-around VSP, with shots made at a constant offset in a 180° or 360° arc (MacBeth, 2001). Various analysis options are available, including AVO, travel time differences (both cumulative from the surface to the receiver and interval measurements between two receiver levels), and also polarization angle differences which exploit the changes in refraction as the azimuthal velocity varies.

A synthetic walk-around VSP is used to analyze the same model that was presented above when discussing AVO (isotropic shale layer over fractured sandstone, here with the fracture strike aligned at N45°E). The shots are located at 15° intervals in a circle at a constant offset of 1000 m from a vertical well, with the geophones positioned at regular intervals through the fractured region. Three methods are used to analyze the first break P-wave arrivals (Figure 7): A, the cumulative travel times at the base of the fractured zone show an elliptical response with the shortest times associated with the direction parallel to the fracture strike; B, the interval travel times between the base and the top of the fracture zone confirm a faster velocity (shorter times) parallel to the fracture strike; and C, the polarization of the P-waves, measured by rotating the three component geophones into the sagittal plane (along source-receiver azimuth), give a decreased refraction of the signal as the velocity slows away from the fracture strike.



Figure

6: Isotropic and anisotropic synthetic gathers computed for PP and PSv reflections from the top of the fractured sandstone (see Figure 5 legend). Tracks show from left to right: Isotropic PP, Anisotropic PP, Isotropic PSv, and Anisotropic PSv gathers. Gathers are computed in 1° increments from vertical incidence out to 30°.

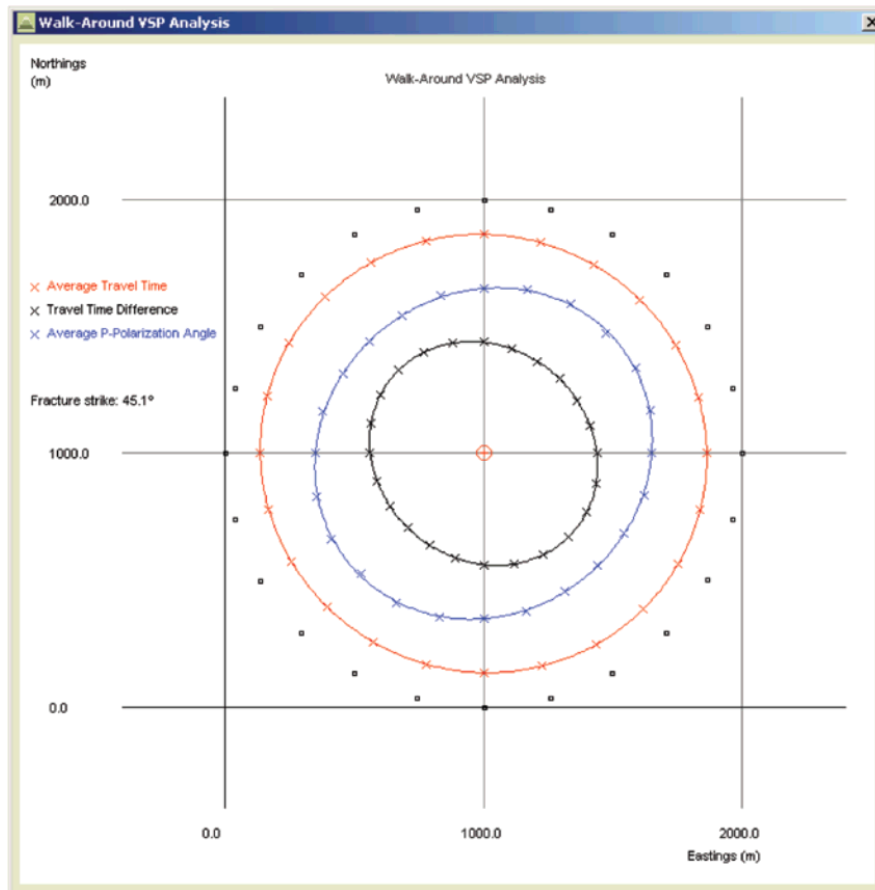


Figure 7: Analysis of the P-wave travel time and P-wave polarization data recorded in a synthetic walk-around VSP from the fracture model used in Figure 5. Curves representing the cumulative first break time (red – shortest times in line with the fracture strike), the difference between first break times recorded at the base and top of the fracture zone (black – again shortest times in line with the fracture strike) and the P-wave polarization angle (blue – angle given with respect to the vertical direction at the top of the fractured sand layer, shows increase at fracture strike direction as the ray is refracted by the faster velocity) are inverted to yield the fracture strike direction (N45°E). The walk-around VSP has shots spaced in a circle every 15° (offset 1000m), shooting into receivers located in a vertical well at the circle's centre.

Fractures -shear-wave splitting

The behaviour of shear-waves as they pass through anisotropic media has been recognized for many years, with laboratory and field observations demonstrating how the shear-wave splits into two polarized components with their planes aligned parallel and perpendicular to the anisotropy. For a fractured medium, the faster shear-wave is generally aligned with the strike direction and the time delay between the split shear-waves related to the fracture density and path length travelled. For layered medium, the shear-wave polarized parallel to the layering (having a stiffer modulus) arrives first.

The dipole sonic logging tool has gained popularity for measuring shear-wave at different orientations in the borehole, and gives useful localized anisotropy information (Esmersoy, 1994). This can be correlated with borehole fracture observations from micro-imaging data, or with shale layering, and also with VSP recordings of shear-wave splitting that extend beyond the well.

A study to characterize fracture directions in this way was made using a near offset, multi-component VSP, which was processed by first rotating the geophone's horizontal components into radial and transverse directions (Wild, et al., 1993). The hodogram (Figure 8) is a useful tool to investigate shear-wave splitting and also to confirm that the components have been correctly

rotated. Trace amplitude samples from the radial trace (horizontal direction) are cross-plotted against the equivalent samples from the transverse trace in time gates of 100 ms. At the P-wave onset, the energy should all be present on the radial trace, however away from the first break, where shears might arrive, splitting is recognized, with the first arrival (shown in red) polarized at approximately 45° from the radial and with a second component arriving some 40 ms later, polarized orthogonally (blue bar). This effect, which is seen over a number of geophones within the fractured zone, correlates well with an azimuthal analysis of micro-imaging data from the same well.

Identification and then analysis of the shear-wave can be particularly difficult due to the dependence on P- to shear-wave mode conversion somewhere in the vicinity of the target zone (shear-wave sources are rare), the swamping of the signal by P-wave multiples, and the uncertainty of the path length. This latter point requires underlining; a long path length through weak anisotropy can produce the same splitting and shear-wave separation as a short path length through strong anisotropy. Two methods to assist in the shear-identification are to measure its velocity, possibly by isolating it from reflected and multiple P-waves, and also to look for evidence of splitting itself.

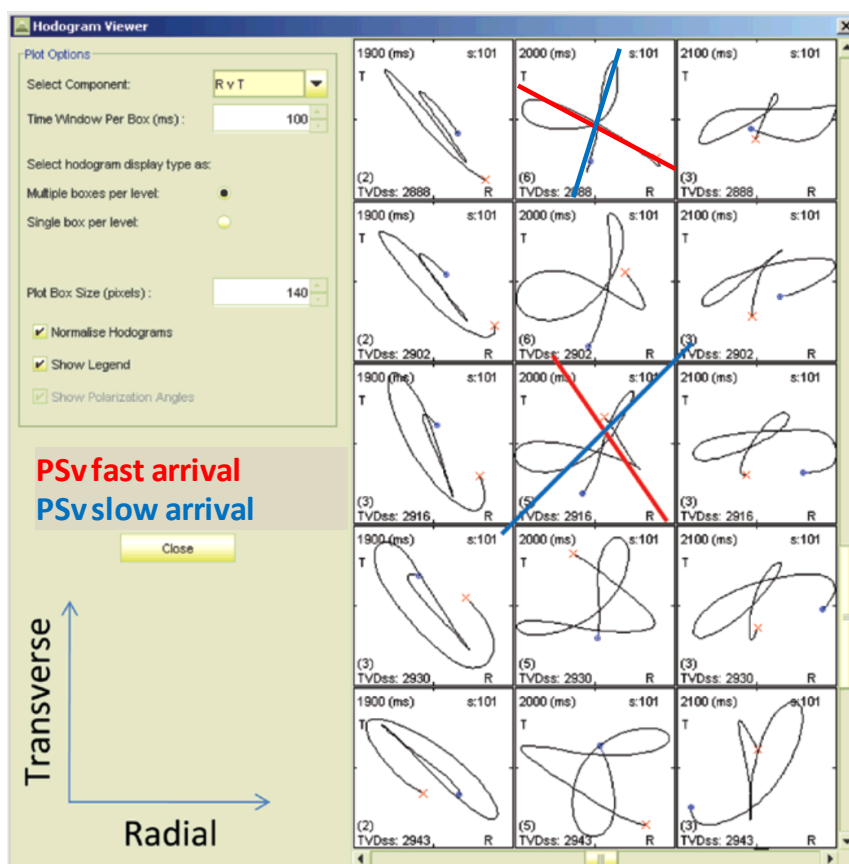


Figure 8: Hodogram plots showing radial versus transverse trace components in 100 ms time gates. The central column (start time = 2000 ms) shows shear-waves that have split into two components, with the first arrival highlighted by the red line in the central plot and the second slower and near-orthogonal arrival (blue line). Measurements indicate that the first shear-wave arrivals are polarized at an angle of approximately 45° from the radial direction.

Tight-gas and shale-gas applications

Several applications of anisotropy to the production of gas from unconventional reservoirs have recently been published. In the development of a tight gas sandstone field in Colorado, Mazumdar and Davis (2010) showed how using shear-waves to image narrow sandstone bodies greatly improved the reservoir imaging, compared to using P-waves; even though the bodies were below

seismic resolution, the increased shear-impedance contrast between sandstone and the surrounding shales demonstrated the value of a 3D shear-wave VSP. In the data processing, azimuthal anisotropy, caused by the fractured sands, was an issue that needed to be rectified prior to pre-stack depth migration of the split shear-wave data, by building azimuthal velocity models to take the azimuthal anisotropy into account. As well as providing an example of anisotropy correction, this study also demonstrated the potential of exploiting the anisotropy, with low regions of shear-wave splitting suggesting evidence of low fracture density which was correlated with the interpretation of micro-imaging data from a nearby well.

A key component for the production of shale gas is stimulated fracturing around horizontal well bores drilled along the shale plays. Close, et al. (2010) provide a useful case study that focuses on the geophysics of shale gas highlighting how anisotropy can be applied to characterize and image these fractures when land-acquired surface seismic data are processed into azimuthal bins and then separately inverted. Regions where the stimulation of fracturing has been successful are shown in the azimuthal interpretation of the seismic data, with the results backed up by simultaneous micro-seismic imaging. Regions where the stimulation has failed are also shown in the seismic and micro-seismic data.

Acquisition design

A requirement is to make decisions regarding the optimum design parameters for seismic acquisition, with the objective of recoding anisotropic information that can be extracted, usually to assess the direction and density of fractures in a reservoir, but also to give information about the overburden that can be included in an anisotropic velocity model. For splitting of converted shear-waves, whether recorded by VSP or OBC, the objective is to have adequate source-receiver offset to ensure that the incoming P-wave will yield a mode-converted shear-wave and to shoot in at least two azimuthal directions, preferably not aligned along or perpendicular to any expected fracture strike.

For a walk-away VSP, the aim is to have a sufficient source offset range to allow slowness values to be computed at angles of incidence as far as possible, bearing in mind that the data quality will deteriorate with longer offsets and that in some situations the first break at a lower receiver might occur before the first break at a higher receiver, due to the faster velocity in lower formations. These so called turning waves will produce a negative vertical slowness and will need special attention in the anisotropy inversion. When inverting walk-away VSPs for overburden anisotropy, it is typical to assume the sub-surface is made up of horizontal layering (VTI anisotropy); here it is important that the walk-away source line is arranged above the receivers or that additional lines are shot when a deviated well makes this impossible to achieve with a single line of shots.

Achieving sufficient coverage in a surface seismic acquisition to give enough fold for full azimuthal processing is expensive, although multiple sail-lines have been used with some success (Li, 1999) and circular shooting makes this a possibility. A more common question is whether fractures can be observed from azimuthal variations in the P-wave AVO signature from a limited number of observation azimuths. Our studies, based on fractured sandstone, carbonate, and granite reservoirs suggest that it is difficult to resolve the azimuthal variations in the P-wave signal against the noise. The anisotropic signal, which increases with offset, is usually less than the 5-10% noise level inherent within the surface seismic data, and the recommendation is that the PS AVO signal is also investigated, if possible, using a VSP or even OBC, where the noise levels are reduced and where there is potential for a greater azimuthal coverage. For the land survey described above for tight gas reservoir characterization, sufficient azimuth and offset ranges were achieved to allow the P-wave AVO signal to be processed and interpreted for fracturing.

Anisotropic models

Before the acquisition feasibility can be fully evaluated, it is necessary to build a model of the anisotropic formations to derive synthetic seismograms at different offsets and azimuths. For layering anisotropy (VTI) there are published studies where the anisotropy has been measured in the laboratory (for example Wang, 2002), which can be used in the model. Empirical studies have also been carried out by fitting velocity data to the anisotropy; one useful paper (Ryan-Grigor, 1997) gives a set of three formula for estimating the three Thomsen (1986) parameters from P- and shear-wave velocities.

For fractured materials (HTI), there is less published laboratory data, but papers by Wang (2002) for sandstones and carbonates and Nur and Simmons (1969) for granites give useful anisotropy benchmark parameters. Two approaches to model fractures have proven useful; Hudson (1981) characterizes the fracturing by aspect ratio and crack density, whereas Schoenberg and Sayers (1995) use compliance values. Although neither aspect ratio nor compliance values are readily available, the latter method of parameterizing the rock is gaining momentum, with a range of techniques to measure fracture compliance being available (see Worthington and Lubbe, 1997, and also below).

Extending published theories to cope with more complex materials, such as fractured layering (orthorhombic symmetry), is possible by fracturing a VTI model with the fractures characterized by their compliance (MacBeth, 2001). In Payne et al., 2010, a procedure is described for building an anisotropic model of a fractured carbonate by combining two pore types, modelled using the theory of Xu and Payne (2009), with fractures added using the compliance methodology of Schoenberg and Sayers (1995). The workflow involves deriving a pore model of the carbonate rock to yield base matrix properties, to which a fracture set is inserted, parameterized using normal and tangential compliances. The compliances were estimated from P-wave velocity data recorded in two wells (one deviated and the other near-vertical) that passed through both fractured and non-fractured portions of the same carbonate formation.

Conclusions

The above applications of seismic anisotropy show where velocity variations caused by anisotropy might be corrected to yield a better well tie, or incorporated into the processing flow for improved imaging. The applications also demonstrate how the measured anisotropy can be exploited, especially to help with fracture interpretation. The past 10 years have seen a number of anisotropic steps routinely incorporated into processing and interpretational workflows. Improved and cheaper logging services makes layering anisotropy information, from dipole sonic measurements in shales and borehole images of fractured formations, more widely available with a larger community keen to exploit this information in their interpretation.

In processing, anisotropic migration formula are available and their effects and requirements more widely understood, especially as ever increasing source-receiver offsets are used.

Based on the recent take up of anisotropy, with supporting software tools and a general understanding of the science, it is highly likely that its application will continue to grow. The means of correcting data for anisotropic velocity is well established, and the use of anisotropy to characterize fracturing and layering is showing its value, especially as unconventional hydrocarbon resources in tight sands and shales become increasingly important. Twenty years ago a session on seismic anisotropy at an international conference was always positioned in the smallest lecture hall at the most inconvenient time. Nowadays the technology is integrated into acquisition, processing,

and interpretational workflows with a widespread take up by both service and oil company sectors of the industry.

References

- Close, D., Striling, S., Cho, D. and Horn, F. [2010] Tight gas geophysics: AVO inversion for reservoir characterisation. *CSEG Recorder*, 35(5), 28–35.
- Esmersoy, C., Koster, K., Williams, M., Boyd, A., and Kane, M. [1994] Dipole shear anisotropy logging. *64th SEG Annual Meeting*, Expanded Abstracts, 1139–1142.
- Grechka, V., Mateeva, A., Gentry, C., Jorgensen, P., Lopez, P. and Franco, G. [2007] Estimation of seismic anisotropy from P-wave VSP data. *The Leading Edge*, 26(6), 756–759.
- Hudson, J.A. [1981] Wave speeds and attenuation of seismic waves in material containing cracks. *Geophysical Journal of the Royal Astronomical Society*, 64, 133–150.
- Jilek, P. [2000] Approximate reflection coefficients of PS-waves in anisotropic media. *70th SEG Conference and Exhibition*, Expanded Abstracts, 19, 182.
- Li, 1999. Fracture detection using azimuthal variation of P-wave moveout from orthogonal seismic survey lines. *Geophysics*, 64, 1193–1201.
- MacBeth, C. [2001] *Multicomponent VSP analysis for applied seismic anisotropy*. Seismic Exploration Series, 26, Pergamon.
- Mazumdar, P. and Davis, T.L. [2010] Shear-wave sourced 3-D VSP depth imaging of tight gas sandstones in Rulison Field, Colorado. *CSEG Recorder*, 35(5), 20–26.
- Nur, A., and Simmons, G. [1969] Stress-induced velocity anisotropy in rock: An experimental study. *Journal of Geophysical Research*, 74, 6667–6674.
- Owusu, J.C., Horne, S.A. and Shabbir, A. [2011] Slowness surface construction and inversion from 3D VSP data. *First Break*, 29(2), 45–50.
- Payne, S.S., Wild, P.W. and Lubbe, R. [2010] An integrated solution to rock physics modelling in fractured carbonate reservoirs. *80th SEG Annual Meeting*, Expanded Abstracts, 358–362.
- Ryan-Grigor, S. [1997] Empirical relationships between transverse isotropy parameters and V_p/V_s : Implications for AVO. *Geophysics*, 62(5), 1359–1364. Schoenberg, M. and Sayers, C. M. [1995] Seismic anisotropy of fractured rock: *Geophysics*, 60(1), 204–211.
- Sheriff, R.E. [2002] *Encyclopedic Dictionary of Applied Geophysics*. 4th Edition, Geophysical References Series 13, Society of Exploration Geophysicists.
- Thomsen, L. [1986] Weak elastic anisotropy. *Geophysics*, 51(10), 1954–1966. Thomsen, L. [2002] *Understanding seismic anisotropy in exploration and exploitation*. SEG-EAGE Distinguished Instructor Series 5. Society of Exploration Geophysicists.
- Tsvankin, I. [2005] *Seismic signatures and analysis of reflection data in anisotropic media*. Second edition. Elsevier Science. Vavryčuk, V. and Pšenčík, I. [1998] PP-wave reflection coefficients in weakly anisotropic elastic media. *Geophysics*, 63(6), 2129–2141.
- Vetri, L., Loinger, E., Gaiser, J., Grandi, A. and Lynn, H. [2003] 3D/4C Emilio: Azimuth processing and anisotropy analysis in a fractured carbonate reservoir. *The Leading Edge*, 22(7), 675–679.
- Wang, Z. [2002] Seismic anisotropy in sedimentary rocks, part 2: Laboratory data. *Geophysics*, 67(5), 1423–1440.
- Wild, P.W., Kemper, M., Lu, L. and MacBeth, C.D. [2008] Modelling anisotropy for improved velocities, synthetics and well ties. *70th EAGE Annual Meeting*, Expanded Abstracts, P235.
- Wild, P.W., MacBeth, C.D., Crampin, S., Li, X-Y. and Yardley, G.S. [1993] Processing and interpreting vector wave-field data. *Canadian Journal of Exploration Geophysics*, 29, 117–124.

Winterstein, D.F. [1990] Velocity anisotropy terminology for geophysicists. *Geophysics*, 55(8), 1070-1088.

Worthington, M.H. and Lubbe, R. [2007] The scaling of fracture compliance. In: Lonergan, L., Jolly, R.J.H., Rawnsley, K. and Sanderson, D.J. (Eds.) *Fractured Reservoirs*. Geological Society, London, Special Publications, 270, 73–82.

Xu, S. and Payne, M., A. [2009] Modelling elastic properties in carbonate rocks: *The Leading Edge*, 28(1), 66–74.
CC02339-MA009 Seabird Exploration.indd 1 08-03-11 09:45